

Gain without inversion in a biased superlattice

F.T. Vasko*

*NMRC, University College Cork, Lee Maltings
Prospect Row, Cork, Ireland*

(Dated: November 14, 2018)

Intersubband transitions in a superlattice under homogeneous electric field is studied within the tight-binding approximation. Since the levels are equi-populated, the non-zero response appears beyond the Born approximation. Calculations are performed in the resonant approximation with scattering processes exactly taken into account. The absorption coefficient is equal zero for the resonant excitation while a negative absorption (gain without inversion) takes place below the resonance. A detectable gain in the THz spectral region is obtained for the low-doped *GaAs*-based superlattice and spectral dependencies are analyzed taking into account the interplay between homogeneous and inhomogeneous mechanisms of broadening.

PACS numbers: 73.21.Cd, 78.45.+h, 78.67.-n

The examination of stimulated emission due to intersubband transitions of electrons (monopolar laser effect), which has been carried out during the previous decade, have resulted in mid-IR lasers (see Refs. in [1, 2]). Recently, the THz laser has also been demonstrated [3, 4, 5, 6]. The standard laser scheme based on vertical transport through the quantum cascade structures, which incorporates the injector and active regions, has been used in both cases. Population inversion appears in the active regions and leads to stimulated emission for the mode propagating along mid-IR or THz waveguide. In contrast to this, the vertical current in a biased superlattice (BSL) with the Wannier-Stark ladder, which appears under the condition $2T \ll \varepsilon_{BB}$ [7] (here ε_{BB}/\hbar is the Bloch frequency and T stands for the tunneling matrix element between adjacent QWs), does not change the populations of the levels. Due to this, the consideration based on the golden rule approach gives a zero absorption. At the same time, for the wide minigap SL, with the width $2T \gg \varepsilon_{BB}$, a negative differential conductivity, i.e. gain due to Bloch oscillations, takes place [8]. This contradiction and the question about THz gain without inversion are discussed in Ref. [9]. Last year, agreement between the numerical results for the wide-miniband and hopping regimes of high-frequency response was noted in [10].

Since there is no well-defined dispersion relation between energy and momentum, ε and \mathbf{p} , beyond the Born approximation, one has to consider the intersubband transitions based on the spectral density function, $A_\varepsilon(\mathbf{p})$, which is a finite-width peak [11]. Let us consider first the two-level model with an identical distribution function for both levels, f_ε . We take into account the off-resonant transitions with a non-zero detuning energy $\Delta\varepsilon = \hbar\omega - \varepsilon_{BB}$ with respect to the level splitting energy, ε_{BB} , see Fig.1. The intersubband absorption is given by

$$\alpha_{\Delta\varepsilon} \propto \int \frac{d\mathbf{p}}{(2\pi\hbar)^2} \int_{-\infty}^{\infty} d\varepsilon A_\varepsilon(\mathbf{p}) A_{\varepsilon-\Delta\varepsilon}(\mathbf{p}) (f_{\varepsilon-\Delta\varepsilon} - f_\varepsilon), \quad (1)$$

moreover the relation $\alpha_{\Delta\varepsilon} \propto \text{sign}(\Delta\varepsilon)$ is obtained under the replacement $\varepsilon - \Delta\varepsilon \rightarrow \varepsilon$. Taking into account that f_ε decreases with ε , one immediately obtains $\alpha_{\Delta\varepsilon} < 0$ if $\Delta\varepsilon < 0$ [12], i.e. a gain appears in the BSL with disorder beyond the Born approximation. In the Born approximation, when the spectral function is replaced by δ -function, one obtains $\alpha_{\Delta\varepsilon} = 0$.

In this paper, we evaluate Eq.(1) for the low-doped BSL taking into account the scattering processes exactly. Numerical estimates are performed below taking into account the interplay between homogeneous and inhomogeneous

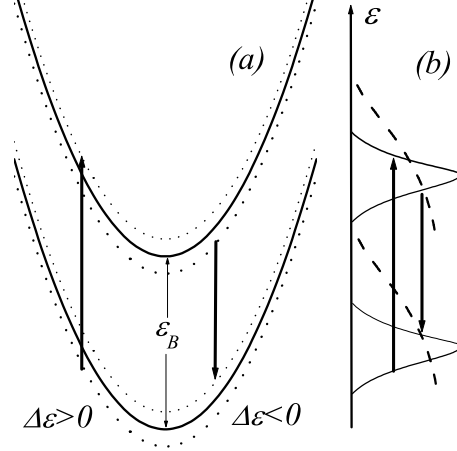


FIG. 1: Off-resonant intersubband transitions (a) and corresponding spectral density functions (b). The dashed curves show distribution functions and arrows indicate the transitions with positive and negative detuning energies.

mechanisms of broadening.

Within the framework of the tight-binding approach we describe the electron states in BSL using the matrix Hamiltonian:

$$\hat{h}_{rr'} = \left(\frac{\hat{p}^2}{2m} + V_{r\mathbf{x}} + r\varepsilon_{BB} \right) \delta_{rr'} + T(\delta_{rr'-1} + \delta_{rr'+1}), \quad (2)$$

where $\hat{p}^2/2m$ is the in-plane kinetic energy operator, m is the effective mass, $V_{r\mathbf{x}}$ is a random potential energy in the r -th QW, $r = 0, \pm 1, \dots$, which are statistically independent in each QW. The Bloch energy, $\varepsilon_{BB} \simeq |e|FZ$, appears in (2) due to the shift of levels in the SL with period Z under a homogeneous electric field F , see [13]. The perturbation operator due to a high-frequency transverse field [$E_{B\perp} \exp(-i\omega t) + c.c.$] is written as $[\widehat{\delta h}_{rr'} \exp(-i\omega t) + H.c.]$, where the non-diagonal matrix $\widehat{\delta h}_{rr'}$ is given by

$$\widehat{\delta h}_{rr'} = \frac{ev_{B\perp}}{\omega} E_{B\perp} (\delta_{rr'-1} + \delta_{rr'+1}) \quad (3)$$

and $v_{B\perp} = TZ/\hbar$. The high-frequency current induced by the perturbation (3), [$I_\omega \exp(-i\omega t) + c.c.$], is determined by the standard formula:

$$I_\omega = i \frac{2ev_{B\perp}}{L^3} \left\langle \left\langle \sum_r \text{sp}_{B\parallel} (\widehat{\delta \rho}_{r+1r} - \widehat{\delta \rho}_{r-1r}) \right\rangle \right\rangle, \quad (4)$$

where 2 is due to spin, $\text{sp}_{B\parallel} \dots$ is the averaging over in-plane motion, $\langle \langle \dots \rangle \rangle$ is the averaging over random potentials $V_{r\mathbf{x}}$, and L^3 is the normalization volume.

The high-frequency contribution to the density matrix in Eq.(4), $[\widehat{\delta \rho}_{rr'} \exp(-i\omega t) + H.c.]$, is governed by the linearized equation:

$$\begin{aligned} & -i\omega \widehat{\delta \rho}_{rr'} + \frac{i}{\hbar} (\hat{h}_r \widehat{\delta \rho}_{rr'} - \widehat{\delta \rho}_{rr'} \hat{h}_{r'}) \\ & + \frac{T}{\hbar} (\widehat{\delta \rho}_{r+1r'} + \widehat{\delta \rho}_{r-1r'} - \widehat{\delta \rho}_{rr'-1} - \widehat{\delta \rho}_{rr'+1}) \\ & + \frac{i}{\hbar} \widehat{\delta h}_{rr'} (\hat{\rho}_{r'} - \hat{\rho}_r) = 0. \end{aligned} \quad (5)$$

Here $\hat{h}_r = \hat{p}^2/2m + V_{r\mathbf{x}} + r\varepsilon_{BB}$ describes an in-plane motion in the r -th QW and we use the steady state density matrix $(\hat{\rho}_o)_{rr'} \simeq \delta_{rr'} \hat{\rho}_r$, i.e. we have neglected a weak non-diagonal term which is responsible for the tunneling

current through the BSL. We restrict ourselves to the consideration of $\propto T^2$ contributions only, so that we can omit $\propto T$ addendums in Eq.(5). Thus, an independent equation for $\widehat{\delta\rho}_r^{\text{B}(\pm)} \equiv \widehat{\delta\rho}_{r\pm 1r}$ takes the form:

$$\begin{aligned} -i\omega\widehat{\delta\rho}_r^{\text{B}(\pm)} + \frac{i}{\hbar}(\widehat{h}_{r\pm 1}\widehat{\delta\rho}_r^{\text{B}(\pm)} - \widehat{\delta\rho}_r^{\text{B}(\pm)}\widehat{h}_r) \\ \simeq -i\frac{ev_{\text{B}\perp}}{\hbar\omega}E_{\text{B}\perp}(\widehat{\rho}_{r\pm 1} - \widehat{\rho}_r). \end{aligned} \quad (6)$$

Note that for the collisionless case $(\widehat{\rho}_{r\pm 1} - \widehat{\rho}_r) \rightarrow 0$, so that the response vanishes and I_ω is only non-zero due to differences in scattering processes for adjacent QWs. In addition, for the resonant approximation, $|\hbar\omega - \varepsilon_{\text{BB}}| \ll \varepsilon_{\text{BB}}$, one can neglect the contribution of $\widehat{\delta\rho}_r^{\text{B}(-)}$.

Writing $\text{sp}_{\text{B}\parallel} \dots$ in Eq.(4) in the coordinate representation, we obtain $I_\omega = (i2ev_{\text{B}\perp}/L^3)\langle \sum_r \int d\mathbf{x} \delta\rho_r^{\text{B}(+) }(\mathbf{x}, \mathbf{x}) \rangle$. Next, we describe the electron states in the r -th QW by the use of the eigenstate problem $(\widehat{p}^2/2m + V_{r\mathbf{x}})\psi_{r\mathbf{x}}^\nu = \varepsilon_{r\nu}\psi_{r\mathbf{x}}^\nu$, where a quantum number ν marks an in-plane state. Using this basis, we transform I_ω into

$$I_\omega \simeq i\frac{2ev_{\text{B}\perp}}{L^3} \left\langle \left\langle \sum_{r\nu\nu'} \delta\rho_r^{\text{B}(+) }(\nu, \nu') \int d\mathbf{x} \psi_{r+1\mathbf{x}}^{\nu*} \psi_{r\mathbf{x}}^{\nu'} \right\rangle \right\rangle \quad (7)$$

and the linearized kinetic equation takes the form:

$$\begin{aligned} (\varepsilon_{r+1\nu} - \varepsilon_{r\nu'} + \varepsilon_{\text{BB}} - \hbar\omega - i\lambda)\delta\rho_r^{\text{B}(+) }(\nu, \nu') \\ = \frac{ev_{\text{B}\perp}}{\hbar\omega}E_{\text{B}\perp}[f_{\varepsilon_{r+1\nu}} - f_{\varepsilon_{r\nu'}}] \int d\mathbf{x} \psi_{r+1\mathbf{x}}^{\nu*} \psi_{r\mathbf{x}}^{\nu'} \end{aligned} \quad (8)$$

Here $\lambda \rightarrow +0$ and we use the quasi-equilibrium distribution $\widehat{\rho}_r = f_{\widehat{p}^2/2m+V_{r\mathbf{x}}}$, where f_ε is the Fermi function with identical chemical potentials, μ , and temperatures, T_e , for any QW. We introduce the conductivity, σ_ω , according to $I_\omega = \sigma_\omega E_{\text{B}\perp}$, and Eqs. (7,8) give us:

$$\sigma_\omega = i\frac{2(ev_{\text{B}\perp})^2}{\omega L^3} \left\langle \left\langle \sum_{r\nu\nu'} \frac{(f_{\varepsilon_{r+1\nu}} - f_{\varepsilon_{r\nu'}})Q_{r+1,r}^{\nu\nu'}}{\varepsilon_{r+1\nu} - \varepsilon_{r\nu'} + \varepsilon_{\text{BB}} - \hbar\omega - i\lambda} \right\rangle \right\rangle, \quad (9)$$

where $Q_{r,r'}^{\nu\nu'} = \left| \int d\mathbf{x} \psi_{r\mathbf{x}}^{\nu*} \psi_{r'\mathbf{x}}^{\nu'} \right|^2$ is the overlap factor. Thus, we have evaluated the expression for the response with the scattering processes exactly taken into account.

Below we consider the absorption coefficient introduced according to $\alpha_\omega = (4\pi/c\sqrt{\epsilon})\text{Re}\sigma_\omega$, where ϵ is the dielectric permittivity, which is supposed uniform across the structure. In order to perform averaging in Eq.(9), we use the spectral density function in the r -th QW determined as $\mathcal{A}_{r\varepsilon}(\mathbf{x}, \mathbf{x}') = \sum_\nu \psi_{r\mathbf{x}}^{\nu*} \psi_{r\mathbf{x}'}^\nu \delta(\varepsilon_{r\nu} - \varepsilon)$ [11], so that $\alpha_{\Delta\varepsilon}$ is written as follows:

$$\begin{aligned} \alpha_{\Delta\varepsilon} = \frac{2(2\pi ev_{\text{B}\perp})^2}{c\sqrt{\epsilon}\omega L^3} \int_{-\infty}^{\infty} d\varepsilon (f_{\varepsilon-\Delta\varepsilon} - f_\varepsilon) \\ \times \int d\mathbf{x} \int d\mathbf{x}' \sum_r \langle \langle \mathcal{A}_{r+1\varepsilon}(\mathbf{x}, \mathbf{x}') \mathcal{A}_{r\varepsilon-\Delta\varepsilon}(\mathbf{x}', \mathbf{x}) \rangle \rangle \end{aligned} \quad (10)$$

with $\hbar\omega \simeq \varepsilon_{\text{BB}}$ in the resonant approximation.

We turn now to averaging over short-range and large-scale potentials taking into account that we are considering SL under a homogeneous bias voltage. Due to this the averaged characteristics of scattering processes, both for homogeneous and inhomogeneous mechanisms, do not depend on the QW number r . It is convenient to use the Wigner representation and the average of the spectral functions in (10) takes the form:

$$\begin{aligned} \int \int \frac{d\mathbf{x}d\mathbf{x}'}{L^3} \sum_r \langle \langle \mathcal{A}_{r+1\varepsilon}(\mathbf{x}, \mathbf{x}') \mathcal{A}_{r\varepsilon-\Delta\varepsilon}(\mathbf{x}', \mathbf{x}) \rangle \rangle \\ = \frac{1}{Z} \int \frac{d\mathbf{p}}{(2\pi\hbar)^2} \langle \langle \mathcal{A}_{r+1\varepsilon}(\mathbf{p}, \mathbf{x}) \mathcal{A}_{r\varepsilon-\Delta\varepsilon}(\mathbf{p}, \mathbf{x}) \rangle \rangle. \end{aligned} \quad (11)$$

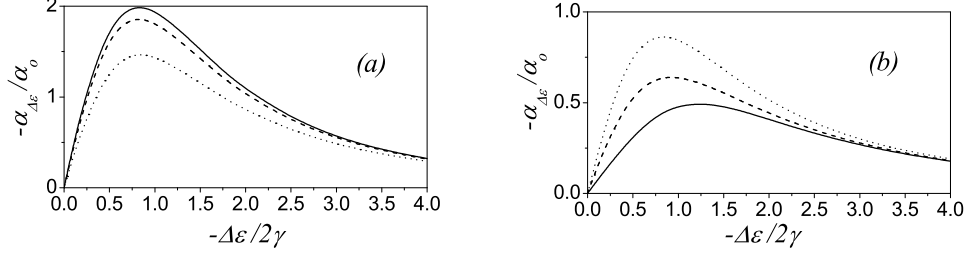


FIG. 2: Dimensionless gain $-\alpha_{\Delta\epsilon}/\alpha_o$ versus detuning energy $-\Delta\epsilon/\gamma$ for the homogeneous broadening case ($\Gamma = 0$). Panels (a) and (b) correspond to degenerate ($\mu/\gamma = 3$) and non-degenerate ($\mu/\gamma = -1$) electrons. Solid, dashed, and dotted curves correspond to $T_e/\gamma = 0.3, 1,$ and 3 respectively.

$T_e/(\gamma, \Gamma)$	$\mu/\gamma=3, \Gamma=0$	$\mu/\gamma=-1, \Gamma=0$	$\mu/\Gamma=3, \gamma=0$	$\mu/\Gamma=-1, \Gamma=0$	$\mu/2\gamma=3, \Gamma=\gamma$	$\mu/2\gamma=-1, \Gamma=\gamma$
0.3	$3.3 \cdot 10^{16}$	$8.8 \cdot 10^{15}$	$4 \cdot 10^{16}$	$1.6 \cdot 10^{15}$	$4 \cdot 10^{16}$	$8.2 \cdot 10^{15}$
1	$3.4 \cdot 10^{16}$	$1.1 \cdot 10^{16}$	$4.1 \cdot 10^{16}$	$5.4 \cdot 10^{15}$	$4.1 \cdot 10^{16}$	$1.3 \cdot 10^{16}$
3	$4.2 \cdot 10^{16}$	$1.5 \cdot 10^{16}$	$5.2 \cdot 10^{16}$	$2.2 \cdot 10^{16}$	$5 \cdot 10^{16}$	$3.4 \cdot 10^{16}$

TABLE I: 3D concentrations, measured in cm^{-3} , versus dimensionless μ and T_e for the cases plotted in Figs.2 ($\Gamma = 0$), 3 ($\gamma = 0$), and 4 ($\Gamma = \gamma$).

Here we took into account that $\langle\langle \dots \rangle\rangle$ does not depend on \mathbf{x} and $L^{-1} \sum_r = Z^{-1}$. Performing the averaging over short-range potential, we write the spectral function $\langle A_{r\epsilon}(\mathbf{p}, \mathbf{x}) \rangle = \text{Im} G_{r\epsilon}^{\text{BR}}(p, \mathbf{x})/\pi$ through the retarded Green's function given by:

$$G_{r\epsilon}^{\text{BR}}(p, \mathbf{x}) = (\epsilon_p - w_{r\mathbf{x}} - \epsilon - \Sigma)^{-1}. \quad (12)$$

Here $w_{r\mathbf{x}}$ is a large-scale part of potential in the r -th QW and Σ is the self-energy function arising from the short-range scattering (see similar calculations in [14]). Below we consider the case of scattering by zero-radius centers when $\text{Im}\Sigma$ does not depend on ϵ, p or \mathbf{x} . $\text{Re}\Sigma$, which is logarithmically divergent without a small-distance cutoff, is included into the detuning energy $\Delta\epsilon$, so that the only homogeneous broadening contribution, $-i\gamma$, appears in the denominator of Rq. (12). Performing the averaging over large-scale potentials we write the spectral density in the integral form:

$$A_\epsilon(\epsilon_p) = \int_{-\infty}^0 \frac{dt}{2\pi\hbar} e^{i(\epsilon_p - \epsilon - i\gamma)t/\hbar} e^{-(\Gamma t/\hbar)^2/2} + c.c., \quad (13)$$

where $\Gamma = \sqrt{\langle w_{r\mathbf{x}}^2 \rangle}$ is the inhomogeneous broadening energy. Using the in-plane isotropy of the problem, we finally transform Eq.(10) into

$$\alpha_{\Delta\epsilon} \simeq \frac{e^2}{\hbar c} \frac{4\pi m v_{\text{B}\perp}^2}{\sqrt{\epsilon} \epsilon_{\text{BB}} Z} \int_{-\infty}^{\infty} d\epsilon \int_0^{\infty} d\xi \times A_{\epsilon - \Delta\epsilon/2}(\xi) A_{\epsilon + \Delta\epsilon/2}(\xi) (f_{\epsilon - \Delta\epsilon/2} - f_{\epsilon + \Delta\epsilon/2}). \quad (14)$$

Note, that for the collisionless case the product of spectral functions under the integrals is transformed into $\delta(\xi - \epsilon + \Delta\epsilon/2)\delta(\xi - \epsilon - \Delta\epsilon/2)$.

Further, we calculate the spectral dependencies $\alpha_{\Delta\epsilon}/\alpha_o$ given by Eq.(14) with the use of the quasi-equilibrium Fermi distribution f_ϵ . The characteristic absorption α_o is introduced here according to $\alpha_o = (e^2/\hbar c) m v_{\text{B}\perp}^2 / \sqrt{\epsilon} \epsilon_{\text{BB}} Z$ and $\alpha_{\Delta\epsilon} = -\alpha_{-\Delta\epsilon}$, so that we consider only the region $\Delta\epsilon < 0$. First, we examine the cases of homogenous ($\Gamma = 0$) and inhomogeneous ($\gamma = 0$) broadening. The dimensionless gain is plotted for the cases of degenerate [Figs.2(a)

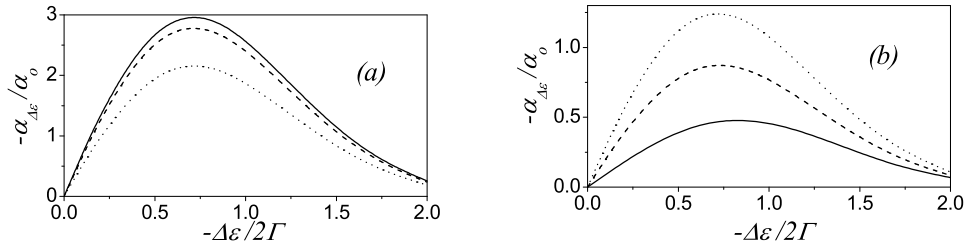


FIG. 3: The same as in Fig.2 for the inhomogeneous broadening case ($\gamma = 0$) depending on parameters μ/Γ and T_e/Γ .

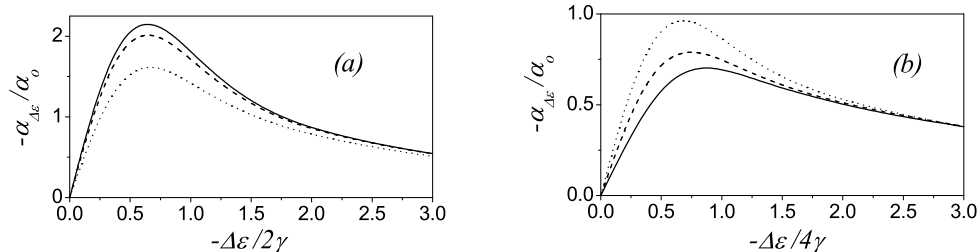


FIG. 4: Dimensionless gain $-\alpha_{\Delta\varepsilon}/\alpha_o$ versus $-\Delta\varepsilon/2(\gamma + \Gamma)$ for the case $\gamma = \Gamma$. Panels (a) and (b) correspond to degenerate ($\mu/2\gamma = 3$) and non-degenerate ($\mu/2\gamma = -1$) electrons. Solid, dashed, and dotted curves correspond to $T_e/2\gamma = 0.3, 1,$ and 3 respectively.

and 3(a)] and nondegenerate [Figs.2(b) and 3(b)] electrons with the concentrations given in Table I. According to these data, concentration increases with T_e for all cases but the peak gain varies in a different manner: quenching or enhancement of gain occurs for degenerate or non-degenerate electrons respectively. High-energy tails of gain and lower peak values take place for the homogeneous broadening case, when (13) has a Lorentzian shape. For the inhomogeneous broadening case, $A_\varepsilon(\xi)$ has a Gaussian shape and $\alpha_{\Delta\varepsilon}$ appears to be a sharper function. In Fig.4 we present the case $\gamma = \Gamma$, plotting the dimensionless gain versus $\Delta\varepsilon/2(\gamma + \Gamma)$, where $2(\gamma + \Gamma)$ is the total width of (13). One can see both the same style of spectral dependencies and the same temperature/concentration dependencies.

Next we turn to estimates of the maximal gain for $GaAs/Al_{0.3}Ga_{0.7}As$ -based BSL with $T = 0.5$ meV, corresponding to the barrier width of 6 nm and $Z = 15$ nm. For the level splitting energy $\varepsilon_{BB} = 10$ meV, which is correspondent to the transverse field $F = 6.7$ kV/cm, one obtains $\alpha_o \simeq 6.6$ cm $^{-1}$, so that the peak gain appears to be between 5 and 20 cm $^{-1}$ for different parameters used in Figs.2-4. Note, that $\alpha_o \propto T^2$ in the framework of the tight-binding approximation and gain increases rapidly for the narrow barrier case, for example gain exceeds the experimental data [3], if $T = 1$ meV.

Let us discuss the main assumptions used. The tight-binding approach is valid under the condition $\varepsilon_{BB} \gg 2T$ which is satisfied for the numerical estimates performed; note, that beyond the Born approximation the broadening can be comparable with the electron energy determined through μ and T_e . We restrict ourselves to the case of homogeneous field and concentration distributions neglecting a possible domain formation due to the negative differential conductivity at low frequencies [15]. One can avoid instabilities in a short enough BSL because the THz modes propagate in the in-plane directions. In spite of the general expressions (10-12) are written through an arbitrary self-energy function Σ , the final calculations were performed for the model included scattering by zero-radius centers and large-scale potential. Such a model describes the interplay between homogeneous and inhomogeneous broadening with the use of statistically independent random potentials in each QW. The Coulomb correlations, which modify the

response as the concentration increases, are not taken into account here. This contribution, as well as consideration of intermediate-scale potential, require a special consideration in analogy with the case of a single QW [16].

In conclusion, we have considered the resonant intersubband response of a BSL and have described gain without inversion beyond the Born approximation. It seems likely that this contribution can be found experimentally and more detailed numerical calculations are necessary in order to estimate a potential for applications.

Acknowledgment: This work was supported by Science Foundation Ireland.

* E-mail: ftvasko@yahoo.com.

On leave from: Institute of Semiconductor Physics, Kiev, NAS of Ukraine, 252650, Ukraine .

-
- [1] C. Gmachl, F. Capasso, D.L. Sivco, and A.Y. Cho, Reports on Progr. in Phys. **64**, 1533 (2001).
- [2] C. Sirtori, F. Capasso, J. Faist, A.L. HutchinsonL, D.L. Sivco DL, and A.Y. Cho, IEEE J. of Quant. Electr. **34**, 1722 (1998); M. Beck, D. Hofstetter, T. Aellen, J. Faist, U. Oesterle, M. Ilegems, E. Gini, and H. Melchior, Science **295**, 301 (2002).
- [3] R. Kohler, A. Tredicucci, F. Beltram, H.E. Beere, E.H. Linfield, A.G. Davies, D.A. Ritchie, R.C. Iotti, and F. Rossi, Nature, **417**, 156 (2002).
- [4] M. Rochat, L. Ajili, H. Willenberg, J. Faist, H. Beere, G. Davies, E. Linfield, D. Ritchie, Appl. Phys. Lett. **81**, 1381 (2002).
- [5] B.S. Williams, H. Callebaut, S. Kumar, Q. Hu, J.L. Reno, Appl. Phys. Lett. **82**, 1015 (2003).
- [6] R. Kohler, A. Tredicucci, F. Beltram, H.E. Beere, E.H. Linfield, A.G. Davies, D.A. Ritchie, S.S. Dhillon, and C. Sirtori, Appl. Phys. Lett. **82**, 1518 (2003).
- [7] S. Ktitorov, G. Simin, and V. Sindalovskii, Sov. Phys. Solid State, **13** 1872 (1971); A. Ignatov and Y. Romanov, Phys. Status Solidi B, **73** 327 (1976).
- [8] Y. Shimada, K. Hirakawa, M. Odnoblioudov, and K. A. Chao, Phys. Rev. Lett. **90** 046806 (2003).
- [9] H. Willenberg, G. H. Dohler, and J. Faist, Phys. Rev. B **67** 085315 (2003).
- [10] A. Wacker, Phys. Rep. **357** 86 (2002), Phys. Rev. B **66** 085326 (2002); in principle, the general formulas presented make possible a description of the gain without inversion for the homogenous broadening case.
- [11] G.D. Mahan, *Many-Particle Physics* (Plenum Press, N.Y., 1990).
- [12] It should be noted that the exact description of scattering processes distinguishes the calculations performed from Ref.9; moreover, the spectral dependencies given by Eqs.(13,14) for the homogeneous broadening case do not coincide with Eqs.(19,24) in [9].
- [13] F.T. Vasko and A.V. Kuznetsov, *Electron States and Optical Transitions in Semiconductor Heterostructures* (Springer, N.Y. 1998).
- [14] F.T. Vasko and E.P. O'Reilly, Phys. Rev. B **67**, 235317 (2003).
- [15] A. Wacker, S.J. Allen, J.S. Scott, M.C. Wanke, A.P. Jauho, Phys. Status Solidi B, **204**, 95 (1997); E. Scholl, *Nonequilibrium Phase Transitions in Semiconductors*. Springer, Berlin, 1987.
- [16] F.T. Vasko, A. Hernandez-Cabrera and P. Aceituno, Phys. Rev. B **66** 125303 (2002); F.T. Vasko, JETP **93** 1270, (2001).